Supporting Information

Vanadium phosphates: exceptionally promising high-voltage cathode materials for future high energy density Mg batteries

Zhen-Dong Huang[a,b,*], Titus Masese[b], Yuki Orikasa[b], Takuya Mori[b], kentarou Yamamoto[b]

[a] Key Laboratory for Organic Electronics and Information Displays & Institute of Advanced Materials(IAM), National Synergistic Innovation Center for Advanced Materials (SICAM), Nanjing University of Posts & Telecommunications, 9 Wenyuan Road, Nanjing 210023, China

[b] Graduate School of Human and Environmental Studies, Kyoto University, Yoshida-nihonmatsu-Cho, Sakyo-ku, Kyoto 606-8501 Japan

Additional experimental information

Preparation and electrochemical delithiation of C-$Li_3V_2(PO_4)_3$ composites

Carbon-coated $Li_3V_2(PO_4)_3$ (C-LVP) was prepared by using the conventional ball-milling assisted carbothermal method. [26] Stoichiometric amounts of LiH_2PO_4 (97%, STREM Chemicals), V_2O_5 (98+%, Sigma-Aldrich) powders corresponding to 0.01 mol of $Li_3V_2(PO_4)_3$, citric acid (anhydrous, Wako) and Ketjen carbon black (KB) were sealed into a zirconia (ZrO_2) pot with 10 ml ethanol and 15.9 g zirconia ball. Subsequently, the mixture was ball-milled on a planetary pulverizer (FRITSCH, Pulverisette 7) at 300 rpm for 10 h with reverse rotation every 15 min. After being dried at 70 ^oC for 10 h, the dried slurry was separated with zirconia ball and pulverized using an agate mortar, thereafter pelletized at 50 MPa using a hydraulic press machine. The pellet was pre-calcined at 300 ^oC for 6 h followed by final calcination at 750 ^oC for 5 h in a tube furnace with a fixed Ar flux. The final product was pulverized by ball-milling at 500 rpm for 12 h.

The as-prepared C-LVP powders were used to prepare the electrodes by mixing the ball-milled active powder with KB and polytetrafluoroethylene (PTFE). The final weight ratio of LVP/C+KB/PTFE was 75:15:10. Subsequently, the obtained sheet was punched into 6 mm discs (the typical mass loading is ~ 3 mg per disc) and pressed between two Pt meshes. The final electrodes were vacuum dried at 70 ^oC for 12 h C-LVP electrodes were electrochemically delithiated in three-electrode Mg cells assembled in an Ar-filled glove box (MIWA) (see the constructions illustrated in Figure S4). Polished Mg rod was used as counter electrode. Ag/Ag^+ electrode prepared by inserting a silver wire into a glass tube containing a solution of 0.1 M $AgNO_3$ in acetonitrile was used as reference electrode. 0.5M $Mg(TFSI)_2$ in acetonitrile (solvent) was used as electrolyte. The solution of 0.1 M $AgNO_3$ in acetonitrile was brought into contact with $Mg(TFSI)_2$/acetonitrile solution via a microporous glass membrane. Electrochemically delithiated $V_2(PO_4)_3$

(ED-VP) was obtained by charging the assembled Mg cells at a current density commensurate to 0.05C (1C = 197 mAh g^{-1}) rate at 55 ºC. The delithiated ED-VP was disassembled from the fully charged Mg cell, followed by washing with acetonitrile for several times. As a control experiment, C-LVP was also delithiated in two-electrode lithium ion cells with Li sheet as anode, microporous polypropylene membrane as separator and 1 mol L^{-3} solution of $LiClO_4$ in ethylene carbonate/diethyl carbonate (1:1 ratio by volume, all received from Kishida chemical) as electrolyte.

Electrochemical characterization

The electrochemical performances of C-LVP and ED-VP as cathode material for Mg battery were characterized in three-electrode cells shown in Figure S4. The protocols for preparation of the electrode and cell assembly were the same as those employed during the delithiation process of LVP. Galvanostatic charge and discharge measurements in an appropriate potential window *vs.* Ag/Ag^+ were carried out at a current density corresponding to 0.05C rate at 55ºC. After being fully charged, the charged C-LVP electrodes were discharged to various capacities corresponding to 39.4 mAh g^{-1}, 78.8 mAh g^{-1}, 118.2 mAh g^{-1}, 157.6 mAh g^{-1} and 197 mAh g^{-1}. The fully charged and discharged electrodes were rinsed several times with super-dehydrated acetonitrile followed by vacuum drying for 12 h. The compositions of discharged LVP were analyzed by using inductively coupled plasma (ICP) measurements. Synchrotron X-ray diffraction (SXRD) and X-ray absorption spectroscopy (XAS) measurements were performed on pristine and charged /discharged C-LVP to assess the crystal and electronic structures after the electrochemical measurement. The cyclic voltammograms during the initial 7 cycles of LVP in three-electrode Mg cells and $V_2(PO_4)_3$ electrodes obtained via the electrochemical delithiation of $Li_3V_2(PO_4)_3$ electrodes (ED-VP) using newly assembled three-electrode cells were performed at a scanning rate of 0.1 mV s^{-1} at 55 ºC, respectively.

Characterization of morphology, crystal structure and Rietveld refinement of synchrotron X-ray diffraction patterns (SXRD)

The morphology of the as-prepared C/LVP was characterized by using scanning electron microscopy (JEOL, JSM-890) at an acceleration voltage of 15 kV. Synchrotron X-ray diffraction patterns of C-LVP were collected at the beam line BL02B2 (SPring-8 in Japan), equipped with a large Debye-Scherrer camera. C-LVP powder and the charged/discharged LVP electrodes were sealed in a glass capillary in an Ar-filled glove box to prevent the sample's exposure to air. To minimise the effect of X-ray absorption by the

samples, the wavelength (λ) of the incident X-ray beam was set to 0.49971(1) Å using a Si monochromator, which was calibrated with a CeO_2 standard. X-ray diffraction data were recorded on an imaging plate for 1 h. The crystal structure was further refined by the Rietveld method with the program JANA2006 using the pseudo-Voigt function of Finger *et al* [1, 2] and drawn by the software of VESTA. [3]

X-ray absorption measurements

X-ray absorption spectra of pristine and charged/discharged LVP electrodes were measured in the energy region of the V-*K* edge at room temperature in transmission mode at the beam line BL14B2 of SPring-8. The intensity of X-ray beam was measured by ionization detectors. Treatment of the raw X-ray absorption data was performed with Athena package. [4] Analysis of V-*K* and Fe-*K* edge XANES spectra was performed with the Rigaku REX 2000 program package. [5]

Table S1. Summary of the reported cathode materials for rechargeable Mg batteries.

Materials and preparation methods	Theoretical capacity / mAh g^{-1}	Discharge capacity / mAh g^{-1}	Discharge current density / mA g^{-1}	Average working voltage *vs*. Mg / V	Ref.
$Li_3V_2(PO_4)_3$ (Solid state reaction)	197 (3e)*	197	9.85	~ 3.0	Present study
$V_2(PO_4)_3$ (Electrochemical delithiation)	208 (3e)*	197	9.85	~ 2.9	Present study
$Cu_yMo_6S_8$ (Partial extraction of Cu from $Cu_2Mo_6S_8$)	114	100	19	~ 1.1	[6]
Mo_6S_8 (Extraction of Cu from $Cu_2Mo_6S_8$)	122	90	15.4	~ 1.1	[7]
$MgFeSiO_4$ (Solid state reaction)	156	125.1	15.6	~ 1.6	[8]
Mesoporous $Mg_{1.03}Mn_{0.97}SiO_4$ (Hard template route)	314	301.4	62.8	~ 1.6	[9]
bulk $Mg_{1.03}Mn_{0.97}SiO_4$ (Solid state reaction)	314	98	62.8	~ 1.6	[9]
$C/Mg_{1.03}Mn_{0.97}SiO_4$ (Sol-gel method)	314	80	12.56	~ 1.6	[10]
$MgCoSiO_4$ (Solvothermal reaction)	305.7	167	30.57	~ 1.8	[11]
$MgCoSiO_4$ (Melten salt reaction)	305.7	123.3	30.57	~ 1.8	[11]
$MgCoSiO_4$ (solid state reaction)	305.7	70.2	30.57	~ 1.8	[11]
VO_x nanotube (hydrothermal reaction)	/	76	5	~ 1.0	[12]
Cu-doped VO_x nanotube (hydrothermal reaction)	/	120	10	/	[13]
V_2O_5 (commercial)	294 (2e)*	153	0.3 mA cm^{-3}	~ 1.35	[14]
V_2O_5 gel/Carbon Composites (Sol casting)	589 (4e)*	589	1000	/	[15]
α-MnO_2 (commercial)	308	280	36 μA cm^{-2}	~ 2.0	[16]
Graphene-like MoS_2 (hydrothermal reaction)	167.5 (1e)* 335 (2e)*	170	20	~ 1.0	[17]
Reduced graphene oxide supported layered MoS_2 (hydrothermal reaction)	167.5 (1e)* 335 (2e)*	104.2	20	~ 1.0	[18]
TiS_2 nanotube (Gas reaction)	240 (1e)*	236	10	~ 1.1	[19]
WSe_2 nanowire(CVD)	235 (3e)*	~220	50	~ 1.5	[20]

**x*e: Number of gained / lost electrons during electrochemical reaction processes.

Table S2. Refined atomic coordinates of $Li_3V_2(PO_4)_3$

atom	*g*	*x*	*Y*	*z*	U_{iso}
Li1	1	0.1133(-)	0.5883(-)	0.1934(-)	0.0263(-)
Li2	1	0.1891(-)	0.1919(-)	0.2599(-)	0.0362(-)
Li3	1	0.4730(-)	0.2213(-)	0.1767(-)	0.0185(-)
V1	1	0.1394(3)	0.5278(2)	0.3903(2)	0.0067(-)
V2	1	0.3612(4)	0.5399(2)	0.1099(2)	0.0065(-)
P1	1	0.0440(4)	0.2502(5)	0.0076(3)	0.0066(-)
P2	1	0.4576(5)	0.3961(4)	0.3508(3)	0.0067(-)
P3	1	0.7524(5)	0.3836(4)	0.1463(2)	0.0063(-)
O1	1	0.0267(10)	0.1747(8)	0.0960(5)	0.0126(-)
O2	1	0.0329(9)	0.3608(8)	0.4233(5)	0.0150(-)
O3	1	0.0844(8)	0.0001(7)	0.2813(5)	0.0102(-)
O4	1	0.1209(9)	0.6351(8)	0.0687(5)	0.0111(-)
O5	1	0.1779(9)	0.7126(9)	0.3184(5)	0.0109(-)
O6	1	0.2380(10)	0.3268(7)	0.0708(5)	0.0112(-)
O7	1	0.2758(10)	0.3860(8)	0.3525(5)	0.0125(-)
O8	1	0.3624(9)	0.5482(7)	0.5411(5)	0.0171(-)
O9	1	0.4761(9)	0.2340(9)	0.3125(5)	0.0099(-)
O10	1	0.5911(10)	0.0185(8)	0.2387(5)	0.0115(-)
O11	1	0.6000(9)	0.4053(7)	0.1676(5)	0.0110(-)
O12	1	0.6748(5)	0.4125(7)	0.0272(9)	0.0128(-)

* *g* and U_{iso} denote the occupancy and isotropic thermal factor, respectively.The atomic positions of Li and isotropic thermal factors (U_{iso}) of atoms were fixed during the Rietveld refinement to the values reported by Kee *et al*. [21]

Table S3. Refined atomic coordinates within the crystal structure of $Li_{0.708}Mg_{0.546}V_2(PO_4)_3$

atom	*g*	*x*	*Y*	*z*	U_{iso}
Li	0.708(-)*	0.278(11)	0.070(10)	0.240(7)	0.003(-)
Mg	0.546(-)*	-0.138(3)	-0.219(2)	0.346(2)	0.003(-)
V1	1	0.142(1)	0.530(1)	0.391(1)	0.003(-)
V2	1	0.356(1)	0.538(1)	0.113(1)	0.003(-)
P1	1	0.031(2)	0.239(1)	-0.007(1)	0.007(-)
P2	1	0.463(2)	0.404(2)	0.352(1)	0.005(-)
P3	1	0.752(2)	0.385(2)	0.151(1)	0.005(-)
O1	1	0.018(4)	0.142(3)	0.062(2)	0.010(-)
O2	1	0.067(4)	0.322(2)	0.403(2)	0.010(-)
O3	1	0.103(4)	0.014(3)	0.289(3)	0.010(-)
O4	1	-0.185(3)	0.645(3)	-0.066(2)	0.010(-)
O5	1	0.165(4)	0.758(3)	0.318(3)	0.010(-)
O6	1	0.437(4)	0.512(3)	0.255(2)	0.010(-)
O7	1	0.289(4)	0.369(4)	0.340(2)	0.010(-)
O8	1	0.376(4)	0.540(3)	0.531(2)	0.010(-)
O9	1	0.499(4)	0.787(3)	0.680(3)	0.010(-)
O10	1	0.834(4)	0.157(4)	0.411(2)	0.010(-)
O11	1	0.587(3)	0.410(3)	0.157(2)	0.010(-)
O12	1	0.668(4)	0.421(3)	0.018(2)	0.010(-)

*$2g_{Mg} + g_{Li} = 1.8$

Table S4. Results of ICP measurements

Sample	Test No.	Li/μg	Mg/μg	V/μg
LVP discharged to 78.8 mAh g^{-1}	1	42.2	41.0	471
	2	42.2	41.3	462
	Average	42.2	41.2	467
LVP discharged to 118.2 mAh g^{-1}	1	44.1	50.1	480
	2	44.9	50	479
	Average	44.5	50	479

Table S5. The calculated lattice parameters of the pristine $Li_3V_2(PO_4)_3$ and the delithiated $V_2(PO_4)_3$ at different discharge state.

Discharge state / mAh g^{-1}	a / Å	b / Å	c / Å	V	β / º
$Li_3V_2(PO_4)_3$	8.6080	8.5939	14.7263	890.4	125.180
39.4	8.5880	8.3341	11.9354	854.0	91.406
78.8	8.6183	8.3565	12.0352	866.7	90.775
118.2	8.6256	8.5982	12.0655	894.8	90.599
157.6	8.7338	8.6502	12.0634	911.2	91.131
197	8.7327	8.4888	11.7774	873.0	90.763

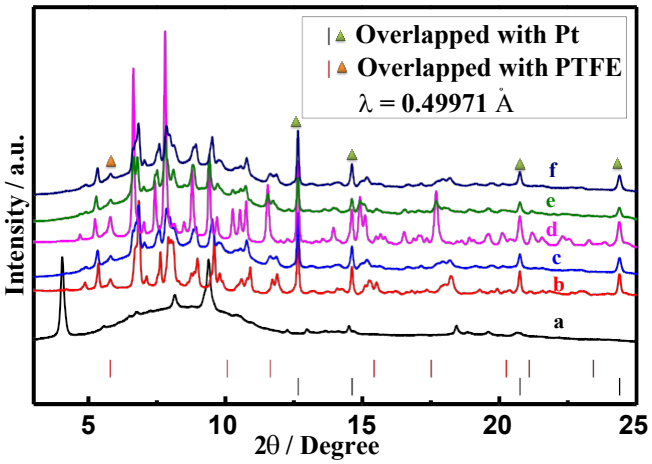

Figure S1. Synchrotron X-ray diffraction patterns of LVP at various states of charge and discharge: (a) 1st charged to 197 mAh g^{-1} (1st C-197), (b) 1st discharge to 39.4 mAh g^{-1} (1st D-39.4), (c) 1st discharge to 78.8 mAh g^{-1} (1st D-78.8), (d) 1st discharge to 118.2 mAh g^{-1} (1st D-118.2), (e) 1st discharge to 157.6 mAh g^{-1} (1st D-157.6) and (f) 1st discharge to 197 mAh g^{-1} (1st D-197).

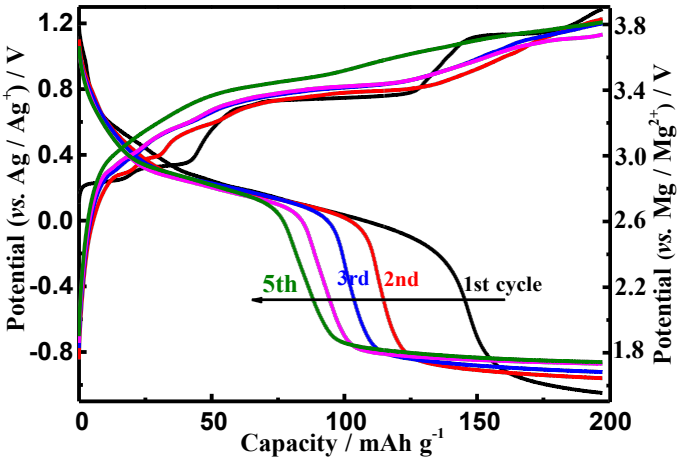

Figure S2. (a) Charge / discharge profiles of LVP in three-electrode Mg cells using Ag/Ag^+ electrode as reference electrode and 0.5 M $Mg(TFSI)_2$ in acetonitrile as electrolyte at a current density of C/20 at 55 °C.

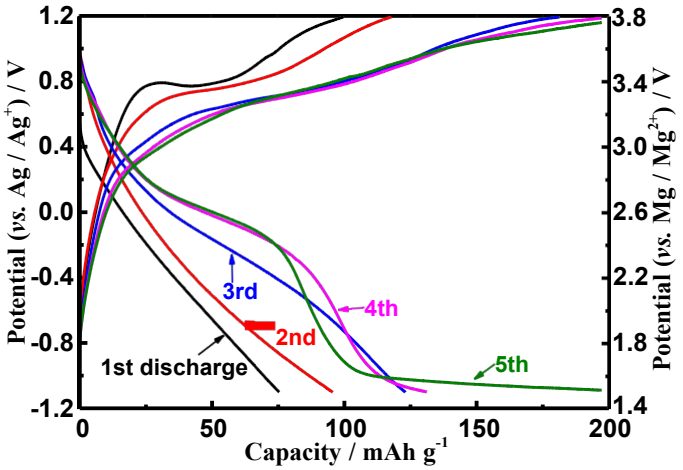

Figure S3. Discharge/charge profiles of $V_2(PO_4)_3$ electrodes obtained via the electrochemical delithiation of $Li_3V_2(PO_4)_3$ electrodes (ED-VP) using newly assembled three-electrode cells at a current density of C/20 at 55 ºC.

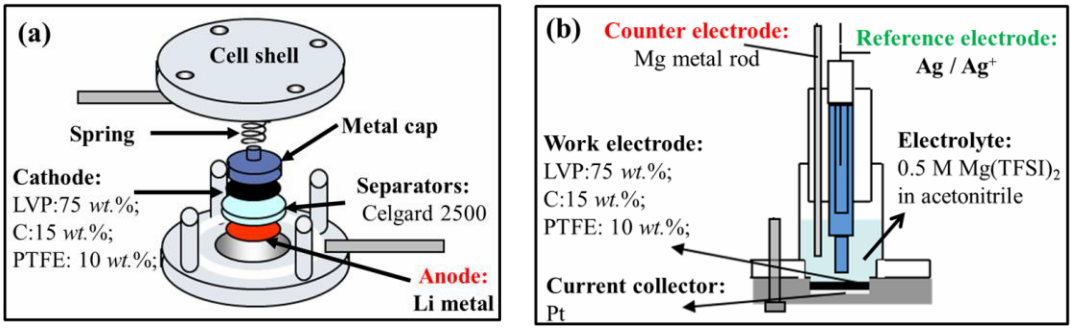

Figure S4. Schematic illustrations of the configuration of the cells used to delithiate $Li_3V_2(PO_4)_3$ and to characterize the electrochemical performance of $V_2(PO_4)_3$ prepared by delithiating $Li_3V_2(PO_4)_3$: (a) two-electrode lithium ion cell and (b) three-electrode Mg cell.

References

1 V. Petrcek, M. Dusek, L. Palatinus, Jana2006-the crystallographic computing system, Institute of Physics, Praha, Czech Republic, **2006**.

2 L.W. Finger, D.E. Cox, A.P. Jephcoat, J. Appl. Cryst., **1994**, 27, 892.

3 K. Momma, F. Izumi, J. Appl. Cryst., **2008**, 41, 653.

4 B. Ravel, M. Newville, J. Synchrotron Rad., **2005**, 12, 537.

5 T. Taguchi, T. Ozawa, H. Yashiro, Phys. Scr., **2005**, T115, 205.

6 A. Mitelman, M. D. Levi, E. Lancry, E. Levi, D. Aurbach, Chem. Commun., **2007**, 4212.

7 E. Lancry, E. Levi, Y. Gofer, M. D. Levi, D. Aurbach, J. Solid. State. Electrochem., **2005**, 9, 259.

8 Y. Li, Y.N. Nuli, J. YANG, T. Yilinuer, J. L. Wang, Chinese Sci. Bull., **2011**, 56, 4.

9 Y.N. NuLi, J. Yang, Y.S. Li and J.L. Wang, Chem. Commun., **2010**, 46, 3794.

10 Z. Feng, J. Yang, Y.N. NuLi, J.L. Wang, J. Power Sources, **2008**, 184, 604.

11 Y.P. Zheng, Y.N. NuLi, Q. Chen, Y. Wang, J. Yang, J.L. Wang, Electrochim. Acta, **2012**, 66, 75.

12 L.F. Jiao, H.T. Yuan, Y.C. Si, Y.J. Wang, J.S. Cao, X.L. Gao, M. Zhao, X.D. Zhou, Y.M. Wang, J. Power Sources, **2006**, 156, 673.

13 L. F. Jiao, H.T. Yuan, Y.C. Si, Y.J. Wang, Y.M. Wang, Electrochem. Commun., **2006**, 8, 1041.

14 L. Yu, X. Zhang, J. Colloid Interface Sci., **2004**, 278, 160.

15 D. Imamura, M. Miyayama, M. Hibino, T. Kudo, J. Electrochem. Soc., **2003**, 150, A753.

16 R.G. Zhang, X.Q. Yu, K.W. Nam, C. Ling, T.S. Arthur, W. Song, A.M. Knapp, S.N. Ehrlich, X.Q. Yang, M. Matsui, Electrochem. Commun., **2012**, 23, 110.

17 Y.L. Liang, R.J. Feng, S.Q. Yang , H. Ma, J. Liang, J. Chen, Adv. Mater., **2011**, 23, 640.

18 Y.C. Liu, L.F. Jiao, Q. Wu, Y.P. Zhao, K. Z. Cao, H.Q. Liu, Y. J. Wang, H.T. Yuan, Nanoscale, **2013**, 5, 9562.

19 Z.L. Tao, L.N. Xu, Xi.L. Gou, J. Chen, H.T. Yuan, Chem. Commun., **2004**, 2004, 2080.

20 B. Liu, T. Luo, G.Y. Mu,X.F. Wang, D. Chen, G.Z. Shen, ACS Nano, 2013, 7, 8051.

21 Y. Kee, H. Yun, Acta Cryst., 2013, E69, i11.